Modeling of Global Processes.
Nonlinear Dynamics and Humanities

Izvestiya Vysshikh Uchebnykh Zavedeniy. Applied Nonlinear Dynamics. 2023;31(3)

Article DOI: 10.18500/0869-6632-003038

Mathematical model of three competing populations and multistability of periodic regimes

B. H. Nguyen, V. G. Tsybulin

Southern Federal University, Rostov on Don, Russia
E-mail: ✉kng@sfedu.ru, vgcibulin@sfedu.ru
Received 30.01.2023, accepted 23.03.2023, available online 27.04.2023, published 31.05.2023

Abstract. *Purpose* of this work is to analyze oscillatory regimes in a system of nonlinear differential equations describing the competition of three non-antagonistic species in a spatially homogeneous domain. *Methods.* Using the theory of cosymmetry, we establish a connection between the destruction of a two-parameter family of equilibria and the emergence of a continuous family of periodic regimes. With the help of a computational experiment in MATLAB, a search for limit cycles and an analysis of multistability were carried out. *Results.* We studied dynamic scenarios for a system of three competing species for different coefficients of growth and interaction. For several combinations of parameters in a computational experiment, new continuous families of limit cycles (extreme multistability) are found. We establish bistability: the coexistence of isolated limit cycles, as well as a stationary solution and an oscillatory regime. *Conclusion.* We found two scenarios for locating a family of limit cycles regarding a plane passing through three equilibria corresponding to the existence of only one species. Besides cycles lying in this plane, a family is possible with cycles intersecting this plane at two points. We can consider this case as an example of periodic processes leading to overpopulation and a subsequent decline in numbers. These results will further serve as the basis for the analysis of systems of competing populations in spatially heterogeneous areas.

Keywords: Volterra model, nonlinear differential equations, competition, family of limit cycles, multistability.

Acknowledgements. The authors are grateful to the referee for careful reading and stimulating comments. The work was carried out at the Southern Federal University with the support of the Russian Science Foundation, grant No. 23-21-00221.

For citation: Nguyen BH, Tsibulin VG. Mathematical model of three competing populations and multistability of periodic regimes. Izvestiya VUZ. Applied Nonlinear Dynamics. 2023;31(3):316–333. DOI: 10.18500/0869-6632-003038

Introduction

Ecological systems are characterized by scenarios of species interaction leading to oscillatory processes. Mathematical modeling of such phenomena is carried out using dynamic systems with continuous and discrete time — flows and cascades [1–5]. For a nonlinear mapping on a segment (in the case of one type), periodic and chaotic dynamics arise, but for a differential equation this is impossible. Oscillatory regimes are observed for two antagonistic species (predator-prey, host-parasite), and only stationary solutions exist for competing populations [6,7]. The question of oscillatory scenarios for three or more non-antagonistic populations is relevant, in particular, for a system with a quadratic right-hand side describing the dynamics of three species [8–17]. In general, this system has eight real parameters ($r_1 = 1$):

$$\dot{u}_1 = r_1 u_1(1 - u_1 - \alpha_1 u_2 - \beta_1 u_3), \tag{1}$$

$$\dot{u}_2 = r_2 u_2(1 - \beta_2 u_1 - u_2 - \alpha_2 u_3), \tag{2}$$

$$\dot{u}_3 = r_3 u_3(1 - \alpha_3 u_1 - \beta_3 u_2 - u_3). \tag{3}$$

Here u_i — the number of the species i, r_i — the growth parameter, the coefficients α_i, β_i characterize the influence of other species on the growth of the species i, and the dot denotes the differentiation in time t.

The system (1)–(3) has zero equilibrium $E_0 = (0, 0, 0)$, three equilibria with one non-zero component

$$E_1 = (1, 0, 0), \quad E_2 = (0, 1, 0), \quad E_3 = (0, 0, 1) \tag{4}$$

and an equilibrium with three non - zero components:

$$E_* = (p_1, p_2, p_3), \quad p_i = \frac{z_i}{z_0}, \tag{5}$$

$$z_1 = \alpha_1\alpha_2 - \alpha_2\beta_3 + \beta_1\beta_3 - \alpha_1 - \beta_1 + 1,$$

$$z_0 = \alpha_1\alpha_2\alpha_3 + \beta_1\beta_2\beta_3 - \alpha_1\beta_2 - \alpha_2\beta_3 - \alpha_3\beta_1 + 1.$$

In (5), the values z_2 and z_3 are obtained from z_1 by cyclic index permutation: $1 \to 2 \to 3 \to 1$.

In a number of works [8–10] the system (1)–(3) was considered with the same growth parameters $r_i = 1$. For the symmetric model ($\alpha_i = \alpha$, $\beta_i = \beta$, $i = 1, 2, 3$) in [8] it is shown that for $\alpha + \beta = 2$ a family of periodic modes on the plane with neutral stability in tangent to the plane direction. In the case of various coefficients $0 < \alpha_i < 1 < \beta_i$, $i = 1, 2, 3$ in [9], the existence of a similar family was established at $A = B$, where

$$A = \prod_{i=1}^{3}(1 - \alpha_i), \quad B = \prod_{i=1}^{3}(\beta_i - 1), \tag{6}$$

In [10], when the conditions $\alpha_i < 1 < \beta_i$ are violated, while maintaining the equality $A = B$, parameter values are found for which there is also a family of periodic modes.

At $r_i \neq 1$, the system (1)–(3) was investigated in [11–17]. So, in [11], the results on calculating the limit cycles for $r_1 = 2$ and $\alpha + \beta > 2$ ($\alpha_i = \alpha$, $\beta_i = \beta$). In [12], using the theorems [13, 14], it is proved that when the condition $A = B$ is met, there is a family of periodic modes for growth parameters r_i, which are expressed in terms of interaction coefficients

$$r_1 = 1, \quad r_2 = \frac{\alpha_1 - 1}{1 - \beta_2}, \quad r_3 = \frac{1 - \beta_1}{\alpha_3 - 1}. \tag{7}$$

In the case of identical growth parameters in [15, 16], a classification of the dynamics of the system (1)–(3) is given. It is shown that there are 37 topological classes defined by the relations between the coefficients α_i, β_i.

In [17] for the system (1)–(3), based on the cosymmetric approach [18], conditions are found under which families of equilibria arise, and oscillatory modes are calculated for parameter values corresponding to the neutral stability of the equilibrium (5). The dynamics under violation of symmetry conditions is analyzed.

The purpose of this work is to analyze the oscillatory modes of the (1)–(3) system and search for families of periodic modes with neutral stability in one direction. In this case, it is assumed that each mode from the family belongs to the corresponding two-dimensional manifold, on which it is the only isolated limit cycle. Thus, this set of periodic modes can be considered a new object - a family of limit cycles. In this paper, a computational experiment is carried out for the system parameters, periods and multipliers of limit cycles are calculated.

1. Investigation of a four-parameter model

[18] describes a scenario for the destruction of a one-parameter family of equilibria of a cosymmetric system, leading to the occurrence of a limit cycle. Let us analyze the possibility of the appearance of a one-parameter family of periodic regimes (limit cycles) with the destruction of a two-parameter family of equilibria. Such a family exists for the system (1)–(3) with $\alpha_i = \beta_i = 1$ and arbitrary values of growth parameters.

Consider the case of a four- parameter model with coefficients $\alpha_i = \alpha$, $\beta_i = \beta$, r_2, r_3. Differential equations (1)–(3) for $\alpha_i = \beta_i = 1$ can be written in vector form:

$$\dot{U} = F, \quad U = [u_1, u_2, u_3]^{\mathrm{T}}, \quad F = P[u_1, r_2u_2, r_3u_3]^{\mathrm{T}}, \quad P = 1 - \sum_{i=1}^{3} u_i. \tag{8}$$

The (8) system has a two-parameter family of equilibria

$$u_1 = 1 - u_2 - u_3, \quad 0 \leqslant u_2 + u_3 \leqslant 1, \tag{9}$$

lying in the plane

$$u_1 + u_2 + u_3 = 1. \tag{10}$$

The stability spectrum of the equilibrium of the family has two zero values $\sigma_1 = \sigma_2 = 0$, corresponding to neutral directions along the plane (10), and the value $\sigma_3 = (1 - r_2)u_2 + (1 - r_3)u_3 - 1$, responsible for stability in the direction transversal to the plane. For any positive values of r_2, r_3, the value of $\sigma_3 < 0$, that is, the whole family consists of stable equilibria. For $r_2 = r_3 = 1$, the spectrum $\sigma_1 = \sigma_2 = 0$, $\sigma_3 = -1$ is identical for all equilibria, which corresponds to the symmetry of the problem, and for $r_2 \neq 1$, $r_3 \neq 1$, each equilibrium has an individual spectrum, which is typical for co - symmetric systems [19].

According to the definition introduced in [19], a cosymmetry is a vector field orthogonal to the field of the problem in the entire space. The two-parameter family corresponds to multicosymmetry, that is, the existence of two different cosymmetries orthogonal to the vector of the right part. The cosymmetries of the (8) system are the vectors introduced in [17]:

$$L_1 = (r_2u_2, -u_1, 0)^{\mathrm{T}}, \tag{11}$$

$$L_2 = (-r_3u_3, 0, u_1)^{\mathrm{T}}, \tag{12}$$

$$L_3 = (0, r_3u_3, -r_2u_2)^{\mathrm{T}}. \tag{13}$$

This is checked directly by calculating the scalar product of the L_i cosymmetry and the right side of the system F.

Since the linear combination of two vectors from (11)–(13) allows you to get a third one (for example, $-u_1 L_3 = r_3 u_3 L_1 + r_2 u_2 L_2$), a pair of cosymmetries can be obtained using the orthogonalization procedure Gram–Schmidt. The resulting vectors will be orthogonal to each other and to the vector of the right side F.

Consider the perturbation of the (8) system with the following choice of interaction coefficients for the original model (1)–(3)

$$\alpha_i = 1 - s, \quad \beta_i = 1 + hs. \tag{14}$$

The method based on the calculation of the cosymmetric defect and the selective function [18] allows analyzing the solutions implemented as a result of the destruction of the family. Scalar products of cosymmetries and vectors of the right side of the system (1)–(3) give cosymmetric defects

$$\mathcal{D}_1 = (F, L_1) = ((u_1 - u_3)\, h + u_2 - u_3)\, s r_2 u_1 u_2, \tag{15}$$

$$\mathcal{D}_2 = (F, L_2) = -\left((u_2 - u_3)\, h - u_1 + u_2\right) s r_3 u_1 u_3, \tag{16}$$

$$\mathcal{D}_3 = (F, L_3) = -\left((u_1 - u_2)\, h + u_1 - u_3\right) s r_2 r_3 u_2 u_3. \tag{17}$$

It can be seen that $\mathcal{D}_i$ vanish for the equilibria E_i(4), as well as for the equilibrium E_*(5), which has three identical coordinates $p_i = [3 + (h-1)s]^{-1}$. Thus, when (14) is perturbed, four equilibria from the two-parameter family are preserved. Let's analyze what happens to the other members of the (9) family. To do this, we substitute in (15)–(17) expressions for the segment of elements (9). As a result, selection (selective) functions are obtained. For example, for the segment $(u_1, u_1, 1 - 2u_1)$, where $0 < u_1 < \frac{1}{3}$, we have:

$$\mathcal{S}_1 = (3u_1 - 1)\,(h + 1)\, s r_2 u_1^2, \tag{18}$$

$$\mathcal{S}_2 = (3u_1 - 1)\,(-1 + 2u_1)\, h s r_3 u_1, \tag{19}$$

$$\mathcal{S}_3 = (3u_1 - 1)\,(-1 + 2u_1)\, s r_2 r_3 u_1. \tag{20}$$

It can be seen that $S_i(u_1) \neq 0$ for any $u_1 \in (0, \frac{1}{3})$. Consequently, when the system (8) is perturbed, only the endpoints remain from the equilibria (9) corresponding to the values $u_1 \in [0, \frac{1}{3}]$. Similarly, it turns out for other segments that go from the point E_* to the boundary of the family of equilibria. In this case, according to [18], limit cycles may appear.

In [8] it is shown that for a symmetric model ($r_i = 1$), a family of limit cycles is obtained at $\alpha + \beta = 2$, which corresponds to the value of $h = 1$. The cycles are located on the plane (10) and form a system of concentric closed curves around the equilibrium (5) with three non-zero components:

$$E_* = \left(\frac{1}{3}, \frac{1}{3}, \frac{1}{3}\right). \tag{21}$$

Let's analyze the properties of these modes for two sets of coefficients: $\alpha = 0.8$, $\beta = 1.2$ and $\alpha = 0.6$, $\beta = 1.4$. In Fig. 1 shows the results of calculations of cycle periods from the family. To do this, the algorithm described in Appendix A is used. In Fig. 1, *a* circles indicate the starting points for calculating periods and multipliers of periodic modes. The trajectory of each mode is determined by the starting point on the plane (10) and does not depend on α, β. The periods of cycles and the values of their multipliers are given in Table. 1. Denote by d the distance from

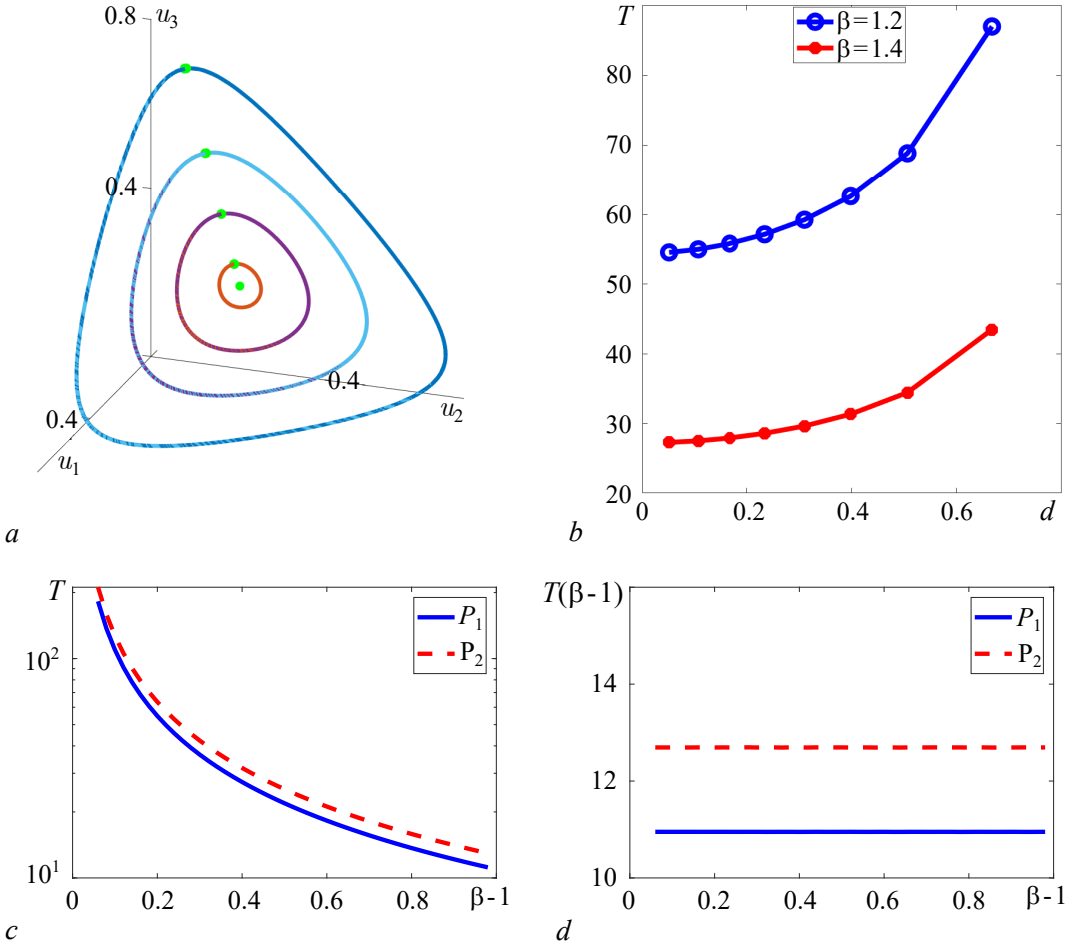

Fig. 1. Family of limit cycles: a — trajectories, b — dependence of period T on the distance from the starting point to equilibrium (21), c and d — graphs dependence of periods of limit cycles on the value of $\beta - 1$ (color online)

the starting point to the equilibrium (21). It can be seen that with an increase in d, the cycle periods grow (рис. 1, b).

In a computational experiment, it was found that with an increase in the difference $\beta-1$, the

Table 1. Periods (T) and multipliers (ρ_i) of limit cycles for $\alpha + \beta = 2$, $r_i = 1$

Interaction coefficients	d	Period	ρ_1	ρ_2, ρ_3
$\alpha_i = 0.8,\ \beta_i = 1.2$	0.05	54.55	1.3×10^{-16}	1.0, 1.0
	0.31	59.25	-1.0×10^{-16}	$1.0 \pm i0.0002$
	0.51	68.87	-1.1×10^{-16}	$1.0 \pm i0.0003$
$\alpha_i = 0.6,\ \beta_i = 1.4$	0.05	27.28	1.4×10^{-12}	1.0, 0.99999
	0.31	29.62	1.4×10^{-13}	$1.0 \pm i6.7 \times 10^{-5}$
	0.51	34.43	1.1×10^{-15}	$1.0 \pm i0.0008$

periods of limit cycles decrease. This is illustrated by Fig. 1, *c*, where the results of calculating the periods of cycles T for two starting points are presented: $P_1 = (0.3, 0.4, 0.3)$ и $P_2 = (0.6, 0.1, 0.3)$. In Fig. 1, *d* the dependencies on $\beta - 1$ of the product $T(\beta - 1)$ are given. Thus, it turns out that the cycle period is inversely proportional to the difference $\beta - 1$, that is, $T = K(\beta - 1)^{-1}$, where K is determined by the choice of the starting point.

The analysis of equilibrium stability and the conducted computational experiment showed that for values other than one r_i on the plane of parameters $\alpha_i = \alpha$, $\beta_i = \beta$ it turns out a map of modes similar to the one given in [8] (fig. 2). For $\alpha, \beta > 1$, there is multistability: the equilibria E_i (4) are stable, and the implementation of a particular equilibrium depends on the choice of the starting point.

The triangle bounded by the segments $\alpha = 0$, $\beta = 0$, $\alpha + \beta = 2$ defines the stability region of the equilibrium E_*(21) at $r_2 = r_3 = 1$. With a change in r_i, the straight line $\alpha + \beta = 2$ turns into a concave curve, so that the stability region of the equilibrium E_* includes a triangle resulting at $r_i = 1$. In this case, the boundary of the deformed region contains a point with coordinates $\alpha = \beta = 1$, for these values, the system (8) has a two-parameter family of equilibria (9) and cosymmetry (11)–(13).

At values α and β outside the stability region of the equilibrium E_* and the multistability zone (stability of the equilibria E_i), a stable heteroclinic cycle [8] is obtained, formed from curves «connecting» the equilibria E_1, E_2 and E_3. The equilibrium data at $\alpha_i < \beta_i$ have one stable and one unstable moustache each, which belong to the planes corresponding to the absence of one of the types ($u_1 = 0$, $u_2 = 0$ или $u_3 = 0$).

In addition, for the four-parameter model ($\alpha_i = \alpha$, $\beta_i = \beta$, r_i), there is a range of values α, β, at which bistability is realized: the equilibrium E_* and the heteroclinic cycle are stable, separated by an unstable saddle limit cycle. In Fig. 2 this region is adjacent to the concave curves — the boundary of the equilibrium stability region E_*.

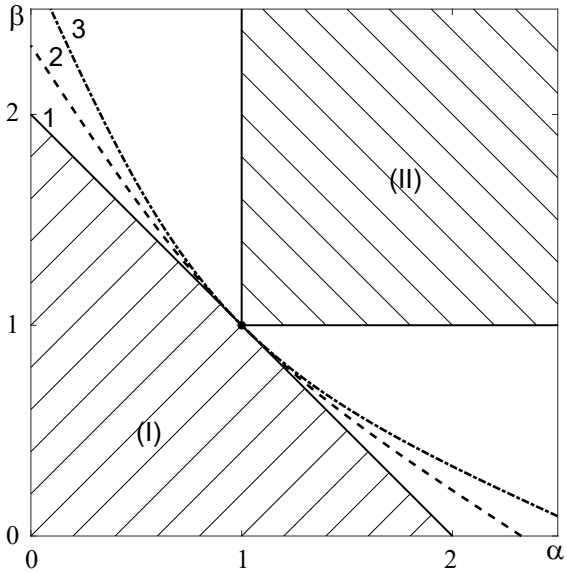

Fig. 2. The stability regions of the equilibria E_* (I) and E_i (II) of the (1)–(3) system for $\alpha_i = \alpha$, $\beta_i = \beta$. Region boundary (I) at $r_2 = r_3 = 1$ (1), at $r_2 = 0.5$, $r_3 = 2.5$ (2), at $r_2 = 2$, $r_3 = 0.2$ (3)

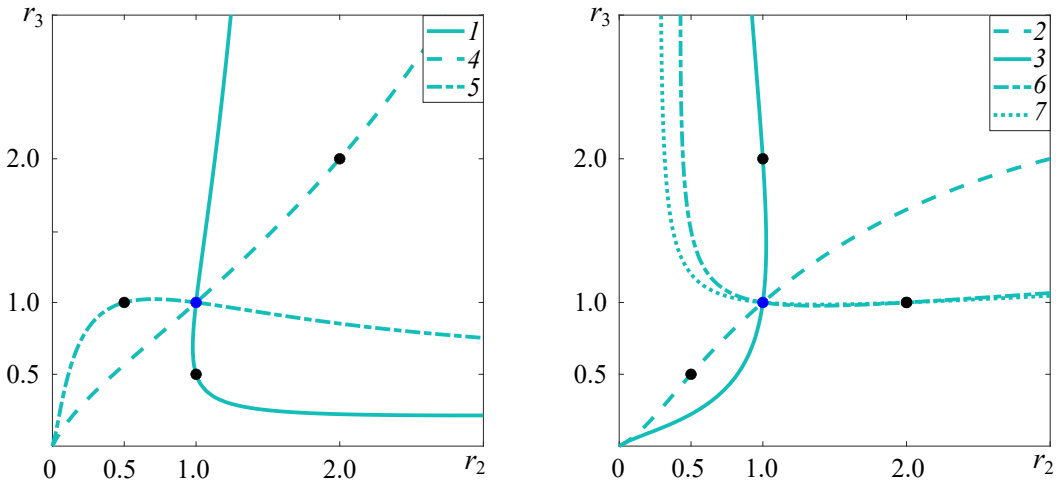

Fig. 3. Dependence curves of r_3 on r_2, which ensure the fulfillment of the condition (23); the numbers correspond to the rows in Table 2 (color online)

2. Computational experiment

To find the limit cycles of the system (1)–(3) with eight parameters, we will analyze the stability of the equilibrium E_*(5), which is determined by the roots of the characteristic polynomial:

$$\sigma^3 + C_2\sigma^2 + C_1\sigma + C_0 = 0, \tag{22}$$

where

$$C_2 = p_1 + p_2r_2 + p_3r_3,$$

$$C_1 = r_2r_3p_2p_3\,(1 - \alpha_2\beta_3) + r_2p_1p_2\,(1 - \alpha_1\beta_2) + r_3p_1p_3\,(1 - \alpha_3\beta_1)\,,$$

$$C_0 = r_2r_3p_1p_2p_3\,(1 - \alpha_1\beta_2 - \alpha_2\beta_3 - \alpha_3\beta_1 + \alpha_1\alpha_2\alpha_3 + \beta_1\beta_2\beta_3)$$

In the work [12] it is shown that an unstable limit cycle exists when the conditions $C_2C_1 > C_0$, $A < B$ are met, and a stable limit cycle is — at $C_2C_1 < C_0$, $A > B$, here A and B are determined by the formulas (6). We will look for parameter values for which the polynomial (22) has a pair of imaginary roots, that is, it is executed

$$C_2C_1 = C_0. \tag{23}$$

The equality (23) contains all eight parameters of the system (1)–(3). In the table. 2 for a number of values of the coefficients α_i, β_i, ensuring the equality $A = B$, the values of the growth parameters r_i are given, for which the existence of families of limit cycles [9, 12] is established. These values of r_i in Fig. 3 correspond to the points through which the curves corresponding to (23). For different variants of α_i, β_i, the curves intersect at a common point $r_2 = r_3 = 1$. Thus, for six sets of interaction coefficients (cases *1–6* from Table. 2) there are families of limit cycles for the growth parameters specified in Table. 2, and for $r_2 = r_3 = 1$. There are also values of the interaction coefficients for which the curve on the plane r_2, r_3 is contracted to a single point. Such a case is given in the last line of the table. 2.

In Fig. 4, *a* presents limit cycles from two families calculated at $\alpha_i = 0.8$, $\beta_1 = 1.1$, $\beta_2 = 1.2$, $\beta_3 = 1.4$, $r_2 = 1$ for the values of $r_3 = 1$ (blue curves) and $r_3 = 0.5$ (red dashed). The starting

Table 2. Combinations of parameters for which there are families of limit cycles under the conditions (23) and $A = B$ (see fig. 3)

α_1	α_2	α_3	β_1	β_2	β_3	r_2	r_3	Кривая
0.8	0.8	0.8	1.1	1.2	1.4	1	0.5	*1*
			1.1	1.4	1.2	0.5	0.5	*2*
			1.4	1.2	1.1	1	2	*3*
			1.4	1.1	1.2	2	2	*4*
			1.2	1.4	1.1	0.5	1	*5*
			1.2	1.1	1.4	2	1	*6*
0.6	0.8	0.9	1.1	1.2	1.4	2	1	*7*
			1.1	1.4	1.2	1	1	

points and the entire family corresponding to the value $r_3 = 0.5$ lie in the plane (10). The limit cycles for the case $r_3 = 1$ intersect the plane (10). As the starting point moves away from E_*, the oscillation amplitude becomes larger. This characterizes Fig. 4, *b*, where graphs of the time variation of the sum of the species are presented $S(t) = \sum_{i=1}^{3} u_i(t)$.

In the conducted computational experiment, it was found that a family of limit cycles exists for r_2, r_3, which differ from those described in [9,12]. In Fig. 5 for the values α_i, β_i corresponding to the cases *1* and *4* from Table. 2, the curve of dependence of r_3 on r_2 satisfying the equality (23) is given. Isolated limit cycles are observed for the values r_2, r_3 lying between this curve (blue solid) and the calculated boundary (red dashed). These modes are located between the heteroclinic cycle and the equilibrium E_*. The points T_j correspond to the values r_2, r_3, at which families of limit cycles are obtained. For example, in the case of *1*, in addition to the points T_1 ($r_2 = r_3 = 1$) [9] and T_2 ($r_2 = 1$, $r_3 = 0.5$) [12], a family of limit cycles is obtained for

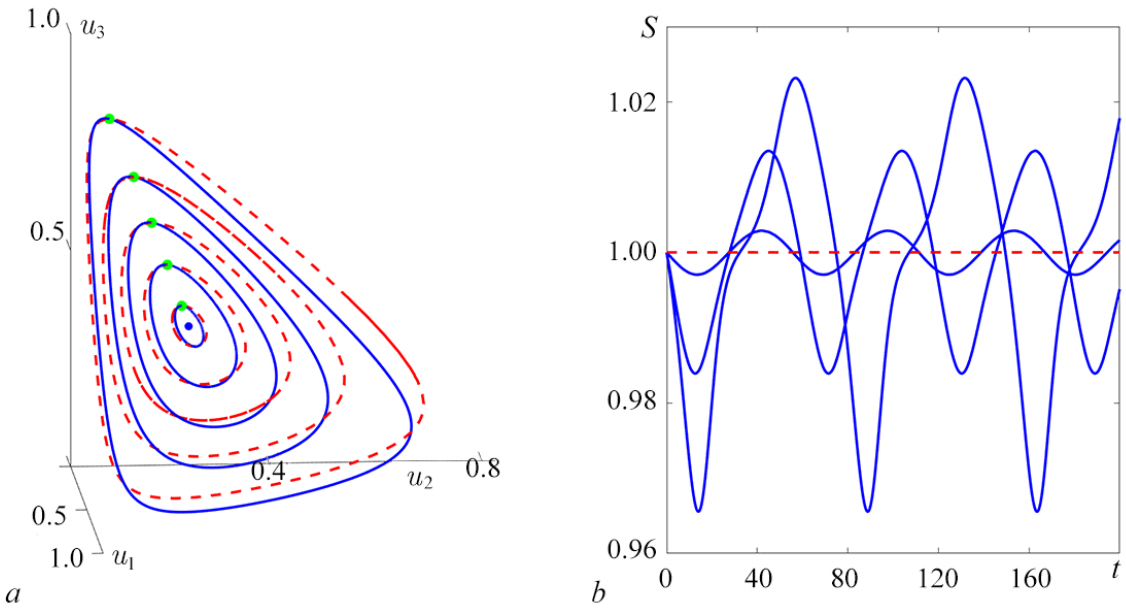

Fig. 4. The family of limit cycles for $r_2 = 1$, $r_3 = 1$ (solid blue lines) and $r_2 = 1$, $r_3 = 0.5$ (red dashed): *a* — trajectories in phase space, *b* — time dependence of the sum of species S; $\alpha_i = 0.8$, $\beta_1 = 1.1$, $\beta_2 = 1.2$, $\beta_3 = 1.4$ (color online)

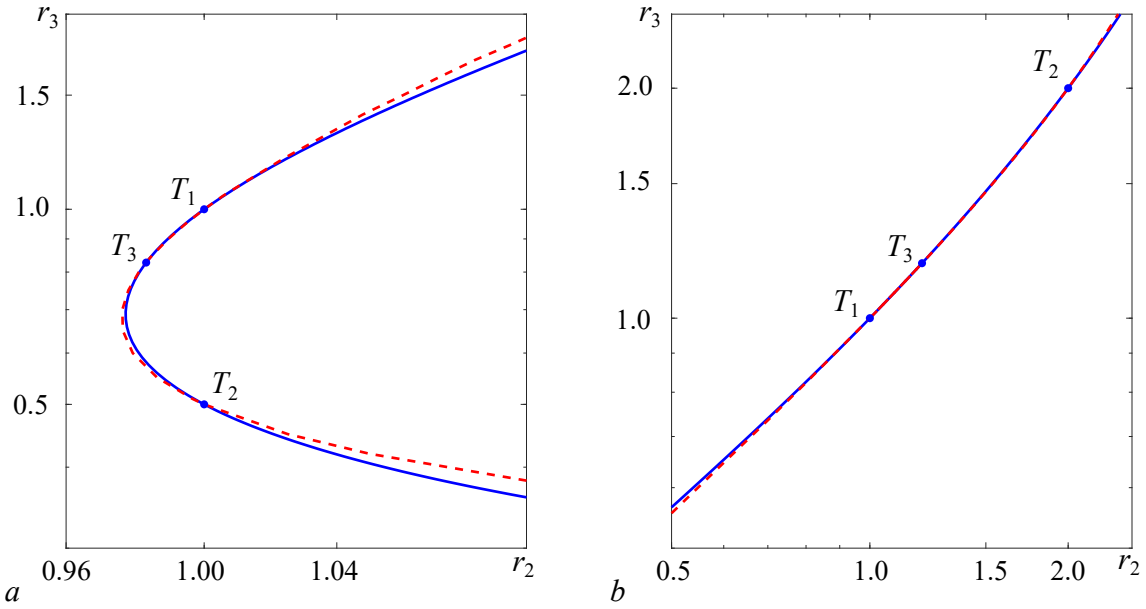

Fig. 5. Curves of dependence of r_3 on r_2 at $\alpha_i = 0.8$, $\beta_1 = 1.1$, $\beta_2 = 1.2$, $\beta_3 = 1.4$ (left) — case *1* in Table 2 and $\alpha_i = 0.8$, $\beta_1 = 1.4$, $\beta_2 = 1.1$, $\beta_3 = 1.2$ (right) — case *4* in Table 2; the blue curve corresponds to (23), the red dashed line marks the boundary of the existence of limit cycles, T_i correspond to families of limit cycles (color online)

Table 3. Period and cycle multipliers for different values of r_2, r_3; $\alpha_i = 0.8$, $\beta_1 = 1.1$, $\beta_2 = 1.2$, $\beta_3 = 1.4$

r_2, r_3	Период	ρ_1	ρ_2, ρ_3
1, 1	58.84	-9.1×10^{-17}	$1.0 \pm i2.4 \times 10^{-5}$
	74.77	6.6×10^{-16}	$1.0 \pm i0.0002$
1, 0.5	75.11	9.2×10^{-18}	$1.0 \pm i0.0004$
	95.4	-1.4×10^{-16}	$1.0 \pm i0.0001$
0.9834636477, 0.8335	59.35	-8.6×10^{-17}	$1.0 \pm i0.0003$
	77.31	1.1×10^{-16}	$1.0 \pm i6.6 \times 10^{-5}$

$r_2 = 0.9834636477$, $r_3 = 0.8335$ (point T_3), see fig. 5, *a*. Note that the points T_j correspond to the intersections of the solid (blue) and dashed (red) curves. From Fig. 5, *b* it can be seen that the range of values r_2, r_3, for which there are isolated limit cycles, can be very small.

Multipliers were calculated for the limit cycles of the family, see Table. 3. It can be seen that the modules of the multipliers ρ_2, ρ_3 are close to one. Under the conditions of the degeneracy of the problem, this can be considered as a good approximation for a two-fold unit, one of which corresponds to the direction along the orbit of the cycle, and the other to the neutral direction for the continuum family.

In Fig. 6 the trajectories of several cycles from the new family are presented ($r_2 = 0.9834636477$, $r_3 = 0.8335$, the point T_3 in Fig. 5, *a*) and convergence of Lyapunov exponents for one cycle from the family.

If the parameters satisfy the condition (23), but at the same time $A \neq B$, then the family of limit cycles degenerates and a slow dynamics is obtained, with a very small increase or decrease

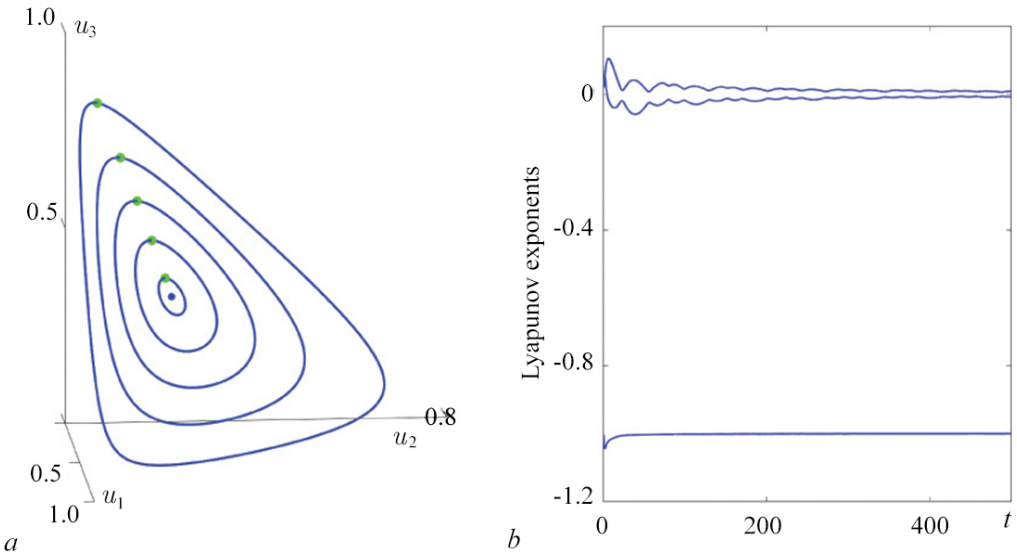

Fig. 6. The family of limit cycles for $r_2 = 0.9834636477$, $r_3 = 0.8335$: a — trajectories in the phase space, b — Lyapunov exponents; $\alpha_i = 0.8$, $\beta_1 = 1.1$, $\beta_2 = 1.2$, $\beta_3 = 1.4$ (color online)

Table 4. Period and multipliers of limit cycles for $A \neq B$; $\alpha_i = 0.8$, $\beta_1 = 1.1$, $\beta_2 = 1.2$

β_3	r_2, r_3	Период	ρ_1	ρ_2, ρ_3
1.45	1.2, 0.22620179898	108.76	-5.8×10^{-18}	1.0, 1.0043
1.35	1.587661492, 3.5	37.8	-1.1×10^{-16}	1.0, 0.99625

in the amplitude of the oscillations. Fragments of such trajectories from a large number of revolutions are presented further in Fig. 7. In this case, it is possible to implement isolated limit cycles. Let's fix the values of five parameters: $\alpha_i = 0.8$, $\beta_1 = 1.1$, $\beta_2 = 1.2$. Then with $\beta_3 = 1.45$ it turns out $A < B$, and with $\beta_3 = 1.35$ — $A > B$. In the table. 4 the multipliers of the calculated limit cycles are presented for different values of r_2, r_3. The first line corresponds to an unstable limit cycle ($\rho_3 > 1$), and the second line corresponds to a stable limit cycle ($\rho_3 < 1$).

The results illustrating the existence of limit cycles are presented in Fig. 7 for a number of values of growth parameters. Calculations were carried out from various initial data (black stars in the figure) at time intervals, allowing to verify the growth or attenuation of the oscillation amplitude (colored stripes in the figure). The end states are marked with blue dots. For $\beta_3 = 1.45$, there are pools of initial data from which the equilibrium E_* and the heteroclinic cycle based on the equilibria E_i are realized (Fig. 7, a). In this case, there is an unstable limit cycle (a thin curve). For $\beta_3 = 1.35$, the equilibrium E_* and the heteroclinic cycle are unstable and there is an isolated limit cycle (Fig. 7, b). This cycle is obtained for small intervals of values of growth parameters r_2, r_3.

In addition, other dynamic scenarios were discovered. For example, with $\beta_3 = 1.45$, $r_2 = 1.6$, $r_3 = 0.195$ and $\beta_3 = 1.35$, $r_2 = 1.6$, $r_3 = 3.62$, there are two isolated (stable and unstable) limit cycles (Fig. 7, c, d). This means bistability in the form of the coexistence of a heteroclinic cycle and an isolated stable limit cycle, as well as equilibrium (stationary solution) and an isolated stable limit cycle. In a computational experiment with fixed interaction coefficients, regions of values of growth parameters are found at which transitions from stable equilibrium with nonzero

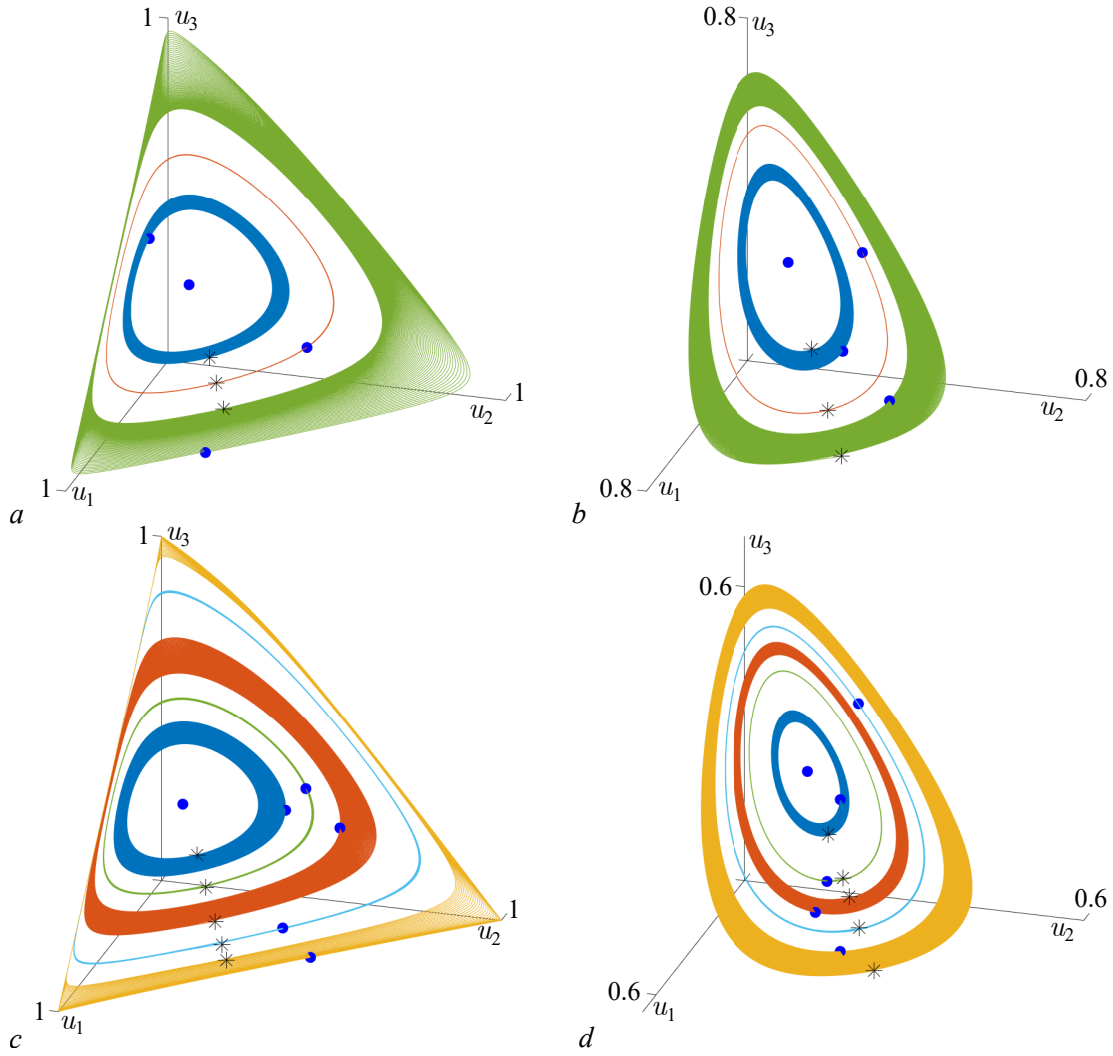

Fig. 7. Oscillations with varying amplitude (color bars) and isolated limit cycles (thin curves) at $\beta_3 = 1.45$ (left) and at $\beta_3 = 1.35$ (right): a — $r_2 = 1.2$, $r_3 = 0.22620179898$, b — $r_2 = 1.587661492$, $r_3 = 3.5$, c — $r_2 = 1.6$, $r_3 = 0.195$, d — $r_2 = 1.6$, $r_3 = 3.62$; initial conditions are black stars, final states are blue dots (color online)

components E_* to a stable heteroclinic cycle are realized. For example, for fixed coefficients $\alpha_i = 0.8$ $(i = 1, 2, 3)$, $beta_1 = 1.1$, $\beta_2 = 1.2$, $\beta_3 = 1.35$ at $r_2 = 1.6$, the equilibrium of E_* is stable from $r_3 \approx 3.7$ to $r_3 \approx 3.6$. For $r_3 \approx 3.62$, stable and unstable limit cycles are born "out of thin air which, with a decrease in the parameter r_3, get into the heteroclinic cycle and the equilibrium E_*, respectively, so that at $r_3 = 3.35$, only the heteroclinic cycle is stable. At values of $0.3 < r_3 < 0.4$, the transition from a stable equilibrium of E_* to a stable heteroclinic cycle occurs with an increase in r_3. A similar scenario is implemented for the values of r_2 close to the considered case $r_2 = 1.6$.

Conclusion

This work is devoted to the study of a relatively simple system of nonlinear ordinary differential equations describing the competition of three non-antagonistic species in a spatially homogeneous area. Oscillatory scenarios of the interaction of species and the emergence of families

of limit cycles are considered. Using the theory of symmetry, a connection is established between the destruction of a two-parameter family of stationary solutions (equilibria) and the emergence of a continuous family of periodic regimes. Earlier in [20, 21] for a system of two predators and prey, a scenario was found for the emergence of a one-parameter family of limit cycles that branch off from the equilibria that make up the one-parameter family. In [22], two-parameter families of equilibria and limit cycles (a consequence of multicosymmetry) were found for a system of two predators and two victims.

The analysis made it possible to find new cases of extreme multistability — the emergence of a continuous family of limit cycles with additional ratios on the system parameters. When these ratios are violated, long-term modes of adjustment to isolated periodic modes, including the heteroclinic cycle, are implemented. Such dynamics is associated with the destruction of a symmetric family of limit cycles.

The results obtained can be useful for analyzing the competition of species taking into account stochastic effects. Practice shows [23–25] that a preliminary study of a deterministic system with the allocation of bifurcation intervals for parameters is useful for interpreting the results taking into account noise. The results shown in Fig. 7, show that for different values of the growth parameters, the phase pattern is significantly changed by small deviations of the coefficient β_3 from the value at which the existence of families of cycles is possible.

Next, it is proposed to study oscillatory modes for spatially distributed systems of competing populations. With $\beta_i = 0$ in [26], a problem for three types is considered, taking into account spatial effects and lag. The analysis of the competition of the two types, taking into account spatial effects, showed that the typical scenario is the establishment of [27] to stationary distributions. With additional relations between the parameters of the systems, co-symmetries and multistable solutions in the form of families of stationary distributions are possible [28, 29].

Application

Calculation of limit cycle multipliers

The system of autonomous differential equations (1)–(3) is written as

$$\dot{u} = f(u), \quad u \in \mathbb{R}^n, \quad u = (u_1, u_2, u_3), \quad n = 3. \tag{24}$$

Its periodic solution having a period $T > 0$ satisfies the condition

$$u(t + T) = u(t). \tag{25}$$

The stability of the periodic solution is determined by the eigenvalues of the monodromy matrix [30, 31], which always has a single eigenvalue $\rho_1 = 1$. If the remaining eigenvalues lie inside the unit circle, then the periodic solution is stable. The solution is unstable if there is at least one eigenvalue outside the unit circle.

In the calculations, an asymptotically stable periodic regime was obtained as a result of the establishment, while the value of the period T was estimated. To calculate the periodic solution of the (24) system, it was assumed that in (25) $t = 0$. After $U_t(x)$, the shift operator along the trajectory of the system is further denoted (24) from the point $u(0) = x$ in time t. The task of finding the limit cycle was reduced to finding the fixed point of the operator $U_t(x)$, that is, the point x satisfying the condition $x = U_T(x)$. The resulting system consisted of n equations with $n + 1$ unknowns (coordinates of the point x and the period T).

$$g(x) = x - U_T(x) = 0, \tag{26}$$

One of the coordinates was fixed in the calculations x ($x_3 \equiv u_3$). Newton's method was used to solve the equation (26)

$$x^{(m+1)} = x^{(m)} - M^{-1}(x^{(m)})g(x^{(m)}) \tag{27}$$

Here M is the Jacobi matrix of the system (26). Together with the solution of the Cauchy problem for (24), problems were solved in variations for which the initial data were the orts of the phase space: $(1,0,0), (0,1,0), (0,0,1)$. At each step of the Newton method (27), the Cauchy problem for the system $n(n+1)$*wassolved* ordinary differential equations. To calculate the limit cycles, various variants of the Runge–Kutta method were used, implemented in MATLAB (functions ode45 and ode89), calculations were performed with absolute and relative accuracy control. In the calculations, the values were used to estimate the convergence of Newton's method 10^{-5} and 10^{-7}, and when calculating by the method Runge–Kutta values were used 10^{-7} and 10^{-9}.

References

1. Svirezhev IM, Logofet DO. Resilience of Biological Communities. Moscow: Nauka; 1978. 352 p. (in Russian).
2. Murray JD. Mathematical Biology. I. An Introduction. New York: Springer; 2002. 551 p. DOI: 10.1007/b98868.
3. Bazykin AD. Nonlinear Dynamics of Interacting Populations. Singapore: World Scientific; 1998. 216 p. DOI: 10.1142/2284.
4. Rubin A, Riznichenko G. Mathematical Biophysics. New York: Springer; 2014. 273 p. DOI: 10. 1007/978-1-4614-8702-9.
5. Frisman YY, Kulakov MP, Revutskaya OL, Zhdanova OL, Neverova GP. The key approaches and review of current researches on dynamics of structured and interacting populations. Computer Research and Modeling. 2019;11(1):119–151 (in Russian). DOI: 10.20537/2076-7633-2019-11-1-119-151.
6. Lotka AJ. Elements of Physical Biology. Philadelphia, Pennsylvania: Williams & Wilkins; 1925. 495 p.
7. Volterra V. Variazioni e fluttuazioni del numero d'individui in specie animali conviventi. Memoria della Reale Accademia Nazionale dei Lincei. 1926;2:31–113 (in Italian).
8. May RM, Leonard WJ. Nonlinear aspects of competition between three species. SIAM Journal on Applied Mathematics. 1975;29(2):243–253. DOI: 10.1137/0129022.
9. Chia-Wei C, Lih-Ing W, Sze-Bi H. On the asymmetric May–Leonard model of three competing species. SIAM Journal on Applied Mathematics. 1998;58(1):211–226. DOI: 10.1137/S0036139994272060.
10. Antonov V, Dolićanin D, Romanovski VG, Tóth J. Invariant planes and periodic oscillations in the May–Leonard asymmetric model. MATCH Communications in Mathematical and in Computer Chemistry. 2016;76(2):455–474.
11. van der Hoff Q, Greeff JC, Fay TH. Defining a stability boundary for three species competition models. Ecological Modelling. 2009;220(20):2640–2645. DOI: 10.1016/j.ecolmodel.2009.07.027.
12. Hou Z, Baigent S. Heteroclinic limit cycles in competitive Kolmogorov systems. Discrete & Continuous Dynamical Systems. 2013;33(9):4071–4093. DOI: 10.3934/dcds.2013.33.4071.
13. Zeeman EC, Zeeman ML. An n-dimensional competitive Lotka–Volterra system is generically determined by the edges of its carrying simplex. Nonlinearity. 2002;15(6):2019–2032. DOI: 10.1088/0951-7715/15/6/312.
14. Zeeman EC, Zeeman ML. From local to global behavior in competitive Lotka-Volterra systems. Transactions of the American Mathematical Society. 2003;355(2):713–734.

DOI: 10.1090/s0002-9947-02-03103-3.
15. Chen X, Jiang J, Niu L. On Lotka–Volterra equations with identical minimal intrinsic growth rate. SIAM Journal on Applied Dynamical Systems. 2015;14(3):1558–1599. DOI: 10.1137/15M1006878.
16. Jiang J, Liang F. Global dynamics of 3D competitive Lotka-Volterra equations with the identical intrinsic growth rate. Journal of Differential Equations. 2020;268(6):2551–2586. DOI: 10.1016/ j.jde.2019.09.039.
17. Nguyen BH, Ha DT, Tsybulin VG. Multistability for system of three competing species. Computer Research and Modeling. 2022;14(6):1325–1342 (in Russian). DOI: 10.20537/2076-7633-2022-14-6-1325-1342.
18. Yudovich VI. Bifurcations under perturbations violating cosymmetry. Doklady Physics. 2004;49(9): 522–526. DOI: 10.1134/1.1810578.
19. Yudovich VI. Secondary cycle of equilibria in a system with cosymmetry, its creation by bifurcation and impossibility of symmetric treatment of it. Chaos. 1995;5(2):402–411. DOI: 10.1063/1.166110.
20. Epifanov AV, Tsybulin VG. Modeling of oscillatory scenarios of the coexistence of competing populations. Biophysics. 2016;61(4):696–704. DOI: 10.1134/S0006350916040072.
21. Epifanov AV, Tsybulin VG. Regarding the dynamics of cosymmetric predator – prey systems. Computer Research and Modeling. 2017;9(5):799–813 (in Russian). DOI: 10.20537/2076-7633-2017-9-5-799-813.
22. Ha TD, Tsybulin VG. Multi-stable scenarios for differential equations describing the dynamics of a predators and preys system. Computer Research and Modeling. 2020;12(6):1451–1466 (in Russian). DOI: 10.20537/2076-7633-2020-12-6-1451-1466.
23. Fay TH, Greeff JC. A three species competition model as a decision support tool. Ecological Modelling. 2008;211(1–2):142–152. DOI: 10.1016/j.ecolmodel.2007.08.023.
24. Bashkirtseva IA, Karpenko LV, Ryashko LB. Stochastic sensitivity of limit cycles for «predator – two preys» model. Izvestiya VUZ. Applied Nonlinear Dynamics. 2010;18(6):42–64 (in Russian). DOI: 10.18500/0869-6632-2010-18-6-42-64.
25. Abramova EP, Ryazanova TV. Dynamic regimes of the stochastic "prey – predatory" model with competition and saturation. Computer Research and Modeling. 2019;11(3):515–531 (in Russian). DOI: 10.20537/2076-7633-2019-11-3-515-531.
26. Bayliss A, Nepomnyashchy AA, Volpert VA. Mathematical modeling of cyclic population dynamics. Physica D: Nonlinear Phenomena. 2019;394:56–78. DOI: 10.1016/j.physd.2019.01.010.
27. Frischmuth K, Budyansky AV, Tsybulin VG. Modeling of invasion on a heterogeneous habitat: taxis and multistability. Applied Mathematics and Computation. 2021;410:126456. DOI: 10.1016/j.amc.2021.126456.
28. Budyansky AV, Tsybulin VG. Modeling the dynamics of populations in a heterogeneous environment: Invasion and multistability. Biophysics. 2022;67(1):146–152. DOI: 10.1134/S0006350922010043.
29. Ha TD, Tsybulin VG. Multistability for a mathematical model of the dynamics of predators and preys in a heterogeneous area. Contemporary Mathematics. Fundamental Directions. 2022;68(3): 509–521 (in Russian). DOI: 10.22363/2413-3639-2022-68-3-509-521.
30. Pontryagin LS. Ordinary Differential Equations. USA: Addison-Wesley; 1962. 304 p. DOI: 10.1016/ C2013-0-01692-1.
31. Waugh I, Illingworth S, Juniper M. Matrix-free continuation of limit cycles for bifurcation

analysis of large thermoacoustic systems. Journal of Computational Physics. 2013;240:225–247. DOI: 10.1016/j.jcp.2012.12.034.